Journal of Power Sources 182 (2008) 546–557

Contents lists available at ScienceDirect

Journal of Power Sources

journal homepage: www.elsevier.com/locate/jpowsour

Robust design of battery/fuel cell hybrid systems—Methodology for surrogate models of Pt stability and mitigation through system controls

Rajeswari Chandrasekaran[a,b,*], Wu Bi[a], Thomas F. Fuller[a,b]

[a] School of Chemical and Biomolecular Engineering, Georgia Institute of Technology, Atlanta, GA 30332, United States
[b] Center for Innovative Fuel Cell and Battery Technologies, Georgia Tech Research Institute, Georgia Institute of Technology, Atlanta, GA 30332, United States

ARTICLE INFO

Article history:
Received 6 February 2008
Received in revised form 12 April 2008
Accepted 14 April 2008
Available online 23 April 2008

Keywords:
PEM fuel cells
Li-ion cell
Hybrid system model
Platinum catalyst degradation
Response surface methodology
Surrogate model
Automobile application

ABSTRACT

With increasing interest in energy storage and conversion devices for automobile applications, the necessity to understand and predict life behavior of rechargeable batteries, PEM fuel cells and super capacitors is paramount. These electrochemical devices are most beneficial when used in hybrid configurations rather than as individual components. A system model helps us to understand the interactions between components and enables us to determine the response of the system as a whole. However, system models that are available predict just the performance and neglect degradation. The objective of this research is to provide a framework to account for the durability phenomena that are prevalent in fuel cells and batteries in a hybrid system. Toward this end, the methodology for development of surrogate models is provided, and Pt catalyst dissolution in proton exchange membrane fuel cells (PEMFCs) is used as an example to demonstrate the approach. Surrogate models are more easily integrated into higher level system models than the detailed physics-based models. As an illustration, the effects of changes in control strategies and power management approaches in mitigating platinum instability in fuel cells are reported. A system model that includes a fuel cell stack, a storage battery, power-sharing algorithm, and dc/dc converter has been developed; and preliminary results have been presented. These results show that platinum stability can be improved with only a small impact on system efficiency. Thus, this research will elucidate the importance of degradation issues in system design and optimization as opposed to just initial performance metrics.

1. Introduction

Environmental pollution not only accelerates climate change but also aggravates serious health concerns, and a major cause is emission from motor vehicles [1]. Pressure from governmental agencies and environmental groups has driven the car manufacturers and energy companies to look for cleaner energy conversion and storage devices. Among the alternatives for transportation are electric vehicles, fuel cell-battery hybrids, and fuel cell–super-capacitor (and battery) hybrids. Neither the fuel-cell hybrid vehicle nor other hybrid vehicles are anticipated to compete with the internal combustion engine on cost or performance alone. Their value is in increasing efficiency and thereby reducing emissions of carbon dioxide.

Hybrid configurations are generally sought to provide both high specific power and specific energy [2–7]. A hybrid configuration is preferred over an all electric or pure fuel cell vehicle in order to combine the advantages of both the technologies and to eliminate their individual disadvantages. A battery is essential in recovering the braking energy, and in providing start-up power, [8] whereas the fuel cell has the principal advantage of being a range extender.

With increasing interest in energy storage and conversion devices for automobile applications, such as rechargeable batteries, proton exchange membrane fuel cells (PEMFCs) and super capacitors, the necessity to understand and predict not just their initial performance but their life behavior is paramount. A system model elucidates the interactions between components, and enables the response of the system as a whole to changing load demands to be determined. However, system models that are available in the literature predict just the performance and do not include the durability and degradation phenomena associated with both fuel cells and batteries.

The main challenges for commercializing PEMFC systems are hydrogen storage, durability, and cost. Durability concerns, such as platinum catalyst degradation [9], carbon catalyst support corrosion [10], and membrane chemical attack [11,12], are key challenges

* Corresponding author at: School of Chemical and Biomolecular Engineering, Georgia Institute of Technology, 311 Ferst Drive, N.W., Atlanta, GA 30332, United States. Tel.: +1 4048942834; fax: +1 4048942866.
E-mail address: rajeswari.chandrasekaran@chbe.gatech.edu (R. Chandrasekaran).

0378-7753/$ – see front matter © 2008 Elsevier B.V. All rights reserved.
doi:10.1016/j.jpowsour.2008.04.038

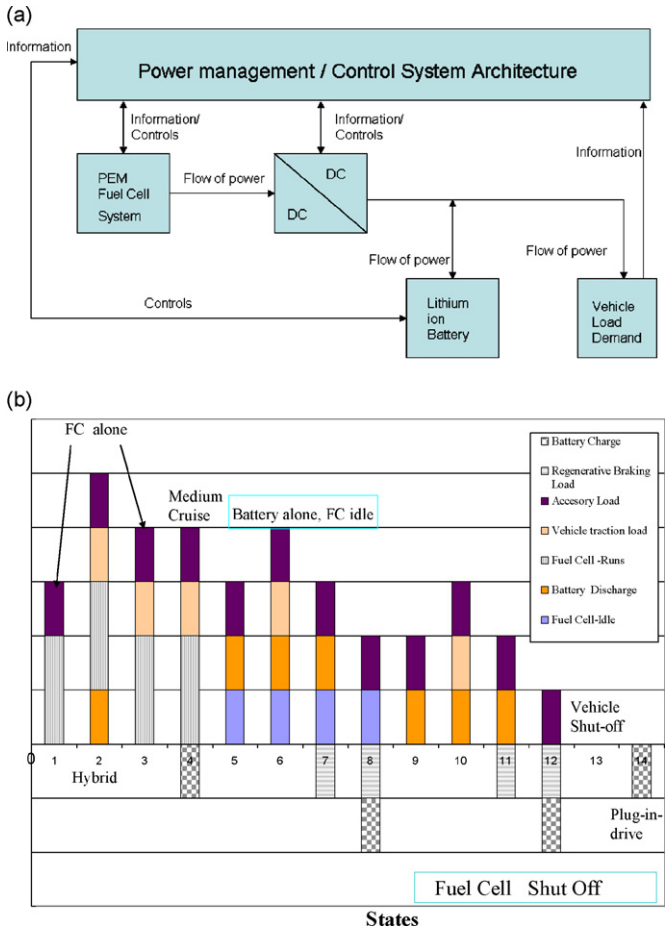

Fig. 1. Structure of the hybrid system. (b) Reasonable states.

[13] because they affect not only the performance of the fuel cell but also the economics and the reliability of the fuel cell technology and its commercialization for automotive applications. Similarly, for secondary batteries, capacity degradation and deterioration in the state of health under both cyclic and storage conditions have to be considered for both long-term safe performance and also life-cycle cost analysis. The aging mechanisms in lithium ion batteries in different components have been extensively discussed in the literatures [14–16].

As illustrated by two recent articles on hybrid vehicle systems, the foremost design goal has been minimizing fuel consumption [17,18]. To their credit, these investigators recognized that multiple objectives must be considered for a robust design. Furthermore, Kim and Peng highlight that the components of the system must be evaluated and the control strategy scrutinized simultaneously. What is missing is any consideration of the durability of the electrochemical devices. Their life and the associated failure mechanisms are strongly dependent on the architecture, load profile, and control strategies.

Furthermore, although efficiency is an important design objective, the small increases in efficiency that are envisaged will have little effect on the commercialization of these fuel-cell hybrid systems. In fact, independent "wells to wheels" analysis by Toyota and Argonne National Laboratory have underscored that efficiency for these systems is only slightly better than an internal combustion engine hybrid. The greater impetus for hydrogen fuel-cells hybrids, plug-in hybrids, or all electric vehicles will be the elimination of the source of carbon dioxide emission from the vehicle. Therefore, reducing the life-cycle cost of the electrochemical storage and conversion devices is the primary technical barrier; and one of the best ways to attack the cost is to improve durability.

Traditionally, durability is not considered in detail until well into the design process. As a result, it is usually too late to account for these phenomena in the design optimization. The flaws in this approach are acknowledged, but there is no established methodology to treat durability of the electrochemical systems in the conceptual design phase in anything more than a superficial manner. This research seeks to change fundamentally this pattern—in short, to develop a framework that allows life or durability constraints of the electrochemical components to be traded against other design objectives, such as weight, efficiency and cost early in the design phase. Similarly, approaches to infuse knowledge about new technologies early in the design phase have been described by Mavris et al. [19]. There are three required elements: (1) development of scalable subsystem models, (2) establishment of framework for design optimization, and (3) creation of surrogate models for degradation phenomena from the detailed physics based models.

A framework is provided that allows designers to explore how changes in hybrid control strategies, system architecture, power management approaches and degree of hybridization impact the degradation of the electrochemical devices. Hence, a robust design methodology allows broader exploration of the design space to arrive at a trade-off between performance metrics—such as hydrogen used, specific energy/specific power, efficiency, cost, size, weight and degradation challenges. To illustrate the methodology, one specific degradation phenomena is considered: platinum stability. For a given driving schedule, the effects of changes in the power sharing between the battery and fuel cell on hydrogen consumption and platinum stability are presented.

2. Baseline fuel cell-battery hybrid vehicle model description

2.1. Vehicle model

The hybrid system conceptualized for this study is shown in Fig. 1 and is comprised of the following subsystems: PEM fuel cell, Li-ion battery pack, dc/dc converter, and power management. A vehicle model (Appendix A) is used to determine the power required to supply the accessories and the electric motor drives, but these devices are not part of the model. In brief, from a prescribed driving schedule, speed *vs.* time, the net power to overcome rolling resistance and aerodynamic drag, accelerate the vehicle, and supply accessories is calculated.

2.2. Fuel cell model

The empirical fuel-cell performance model [20] of Kim et al.,

$$E = E_o - b \ln i - Ri - m\exp\{ni\}, \quad (1)$$

has been fitted to experimental data from our research group that are representative of typical fuel cell performance. The corresponding parameters used in this study are provided in Table 1. Future work will provide these parameters as a function of temperature and reactant pressures. Appendix B gives fuel-cell system design specifications.

A fuel-cell subsystem, consists of an air compressor, humidifier, radiator and hydrogen tanks, is required to supply reactants and control the temperature of the cell stack. The subsystem requires electrical power for its operation, which is usually provided by the fuel-cell system itself. The presence of these subsystems also implies additional mass and consequently less specific energy of

Table 1
Parameters for the PEMFC empirical equation

Parameters	Units	Value
E_0	mV	1128.4602
R	Ohm cm^2	0.0692
b	mV	61.1344
m	mV	7.6401
n	cm^2 mA^{-1}	0.0003

the fuel cell system. Whereas the mass of the subsystem is included, their impact on system efficiency is not accounted for here. A constant accessory power level has been assumed. Hydrogen utilization is assumed to be constant (90%) when calculating the hydrogen used under given driving conditions, and it acts simply as a scaling factor (see Appendix B). The fuel-cell system efficiency, thus, in the present model is a function of the potential of the fuel cell only.

2.3. Battery model

Fellner and Newman's [21] simplified battery model is used. It assumes that the system is ohmically limited, resulting in a linear relationship between the over potential and the current segment. This is a reasonable assumption for hybrid vehicle system where short current pulses are demanded; but as the reliance on the battery increases, this assumption is less appropriate. The capacity of each electrode is updated using Faraday's law.

It is understood that the battery will have an effective thermal management system, and hence this is not dealt with in detail in this study. In the present work, the open-circuit potential as a function of state of charge for the $LiMn_2O_4$ (positive) [22] and carbon (negative) [23] electrodes are estimated from the literature.

Depending on the power demanded, the state of charge (SOC) of the battery, and the power management algorithm (including voltage restrictions), the response of the battery is determined. The charging rate is limited to the *C* rate. Though the chances of the battery going to constant-voltage charge mode may be small in hybrid operation, the model still allows for constant voltage (CV) charging when required.

The SOC can be estimated by counting the coulombs passed (current and time) or from the open-circuit potential, whereas the model needs individual intercalation co-efficients to determine the limiting electrode to calculate the overall capacity of the battery at each time step. For the present study, the battery consisted of 25 Ah lithium ion cells connected in series. Appendix C provides the battery design specifications and model equations including the conversion of SOC to the individual electrode intercalation co-efficients and vice versa. SOC is difficult to determine accurately in the vehicle and is a source of uncertainty. The surrogate model methodology described in this paper can be used to arrive at a robust design that is less sensitive to this uncertainty.

2.3.1. DC/DC converter model

The dc/dc converter efficiency is the ratio of output power to input power. A sixth order polynomial equation was fitted in this proposed work for the dc/dc converter performance curve obtained experimentally by Pei et al. [24] and used in this system model. This is provided in Appendix D.

2.4. Power sharing algorithm of the baseline model

In order to develop a power management algorithm, the different conditions of the individual components have to be identified. These conditions then determine the possible states of the hybrid system. The major components and the conditions considered for the algorithm are shown in Table 2. Of the 54 permutations, just 14 reasonable states emerged as shown in Fig. 1b. For instance, a situation that simultaneously uses the fuel cell and regenerative braking to charge the battery is not considered. It is assumed that whenever the vehicle is on, there is some nonzero net load, *i.e.,* the accessories load is always required.

Table 2
Different possible conditions of the individual components

Battery	Fuel cell	Traction load	Accessory load
Charge	Runs	Traction	On
Idle	Idle	Zero	Off
Discharge	Off	Regenerative braking	

The transition between these different states in the power sharing algorithm is based on the traction load power demand, accessories power demand, battery state of charge and voltage limits, and the rated fuel cell power (maximum power from the fuel cell) as well as the minimum power permitted. This minimum fuel-cell power is established as that power level below which leads to an unacceptably low fuel-cell system efficiency. As will be demonstrated later, there is another perspective to consider when establishing this minimum power. As we operate the fuel cell at lower current densities, the corresponding potential of the fuel cell will increase and approach the open-circuit value. This higher potential will accelerate platinum catalyst dissolution and carbon catalyst support corrosion in the fuel cell stack.

The power sharing algorithm is developed for three cases:

- Traction power demand is greater than or equal to zero, and accessories power demand is positive.
- Traction load is negative, and accessories power demand is positive.
- Both the traction and accessories power demand is zero.

As seen from Table 2, the above cases arise from the reasonable combination of the individual conditions of traction load and accessories load.

In the first case, both the fuel cell and the battery provide power, and the balance between them depends on the SOC of the battery. Whereas in the next case, if its SOC is low, the battery is charged with power from regenerative braking. The third case corresponds to when the vehicle power demand is zero, and so it is either at a standstill – where all energy sources are shut-off – or using the plug-in-drive mode, where the battery is getting charged from an external source. For the baseline model, a constant positive accessories load demand is assumed. The power sharing algorithm for this case is given in Appendix E.

2.5. Influence of control algorithms

The control algorithm establishes the power sharing between the fuel cell and battery and also influences their life-time. The effect on the fuel-cell catalyst stability is addressed in this paper—future work will investigate other fuel-cell and battery degradation mechanisms.

When the power demanded by the vehicle from the fuel cell is zero, the fuel cell can be put in a variety of conditions: (1) open circuit with reactants still provided (idling), (2) operating to supply just enough power for the balance of plant (BoP), (3) completely shut-off, including BoP components, or (4) an off state where some of the BoP components are turned off and the others are powered from the battery. This choice would in turn determine the poten-

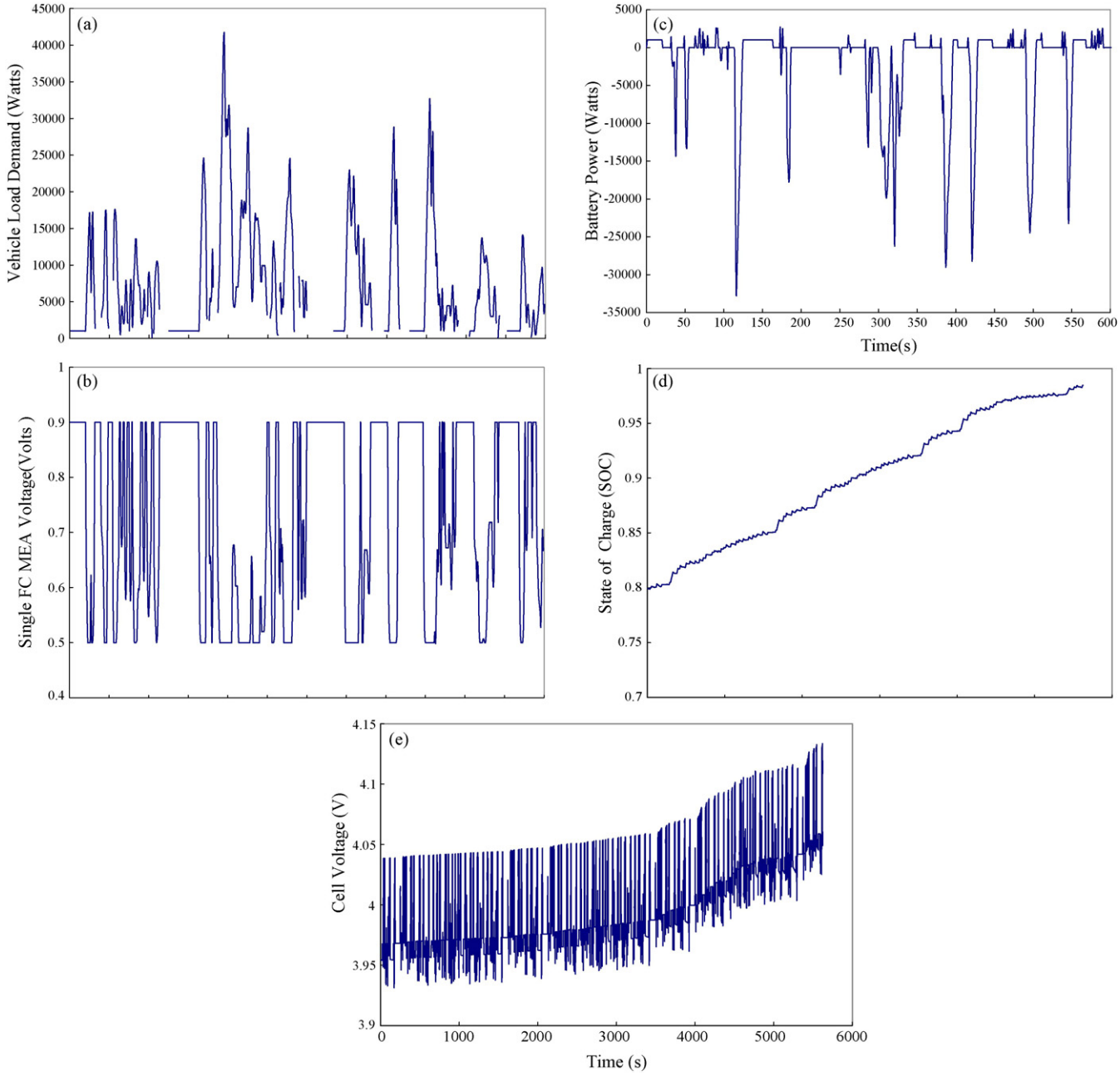

Fig. 2. Baseline model results.

tial window of the fuel cell cycling and thus affect the degradation phenomena in the fuel cell.

The upper fuel cell voltage limit determines the lower power limit for the fuel cell operation. The upper fuel cell voltage could be set at different levels, for example, 0.8 or 0.9 or 1 V. The lower limit of fuel cell potential is set such that mass transfer losses are minimized by avoiding excursions to higher current densities. Under the present control strategy, the higher the upper voltage limit of the fuel cell, the higher the rate of platinum catalyst degradation. If the upper voltage limit is lowered, the fuel cell would be operating less efficiently and negate one of its key advantages. First the results from the baseline model are presented, and then in Section 4 the influence of control algorithm on fuel cell durability and hydrogen consumption are discussed.

3. Baseline model results

3.1. Vehicle model

Baseline results are developed for a fuel cell rated at 90 kW and a 20-kW battery. Thus, the maximum power for the vehicle is 110 kW. The battery consists of 53 lithium ion cells of 25 Ah connected in series. The mass of each lithium ion cell is 0.908 kg. The voltage range of the battery pack is 146–217 V, and that of the fuel stack is 214–427 V. The total power demanded based on the Federal Test Procedure (FTP) driving cycle [25] is computed from the vehicle model. This FTP was intended to represent typical driving patterns in primarily urban areas. The simulation was done for 5624 s, which is the time required for going through the FTP cycle thrice, and

thus ensures that there is sufficient time for noticeable initial rates of degradation in the cell stack to be established. Fig. 2a shows the vehicle load demand for a portion of the schedule for better readability. The power profile is lower than 110 kW range because of the relatively mild driving conditions.

3.2. Power sharing

Fig. 2b shows the voltage profile of a single fuel cell for the baseline control algorithm. Fig. 2c shows the corresponding battery power. Due to mild driving conditions, initial SOC of the battery chosen for this simulation (0.8), and the control algorithm, the battery predominantly gets charged, which is evident from the SOC profile seen in Fig. 2d. The initial SOC of the battery was chosen as 0.8 because it is reasonable to assume that the battery is left at a SOC that is sufficiently high to allow hybrid drive conditions even early in the driving schedule. The control algorithm can handle any SOC value as input parameter; however, choosing a value of 0.8 resulted in a negligible change in the SOC over the selected driving schedule, thus simplifying the efficiency comparisons between control strategies. But in the long run, the chosen power management strategy will decide if a net neutral SOC is obtained. Also if the initial SOC chosen is different, then again net neutral SOC need not be obtained. In these cases, adjustments will have to be made to account for the net change in SOC before proceeding to compare between different control strategies. The potential of the lithium ion cell, seen in Fig. 2e (for the entire time span), is obtained from the difference between the open circuit potential and the over potential of the battery.

4. Proof of concept for the need for robust design

To understand better how different power management algorithms affect efficiency and durability, the allowed upper potential of the fuel cell was varied. The responses (loss terms) *vs.* hydrogen used (kg) for the prescribed driving schedule are plotted in Fig. 3.The Pt surface area loss rate and the radius growth rate shown in the figure are simply the net change in the variable divided by the elapsed time. Pt mass loss rate is further normalized with respect to the MEA area. Fig. 3 shows that as the upper potential is lowered, the hydrogen required increases (because of lower fuel-cell efficiency). At the same time, the rate of Pt degradation is reduced dramatically. If one were to extrapolate the results for a 5000-h driving cycle, it is observed that Pt surface area loss is the dominant issue in catalyst durability. For the case with fuel cell upper potential of 0.9 V, extrapolation to 5000 h is not meaningful, and longer simulations would be required to account for the fact that the rate of surface area loss will decrease over time. For the ranges of upper potential examined, there is an imperceptible Pt mass loss. It is expected that if start–stop losses were also treated, or if the upper potential were raised further, platinum mass loss from the electrode would be significant. Most important, these results provide the framework to make trade-offs between performance and durability. They signify the need to have robust design methodologies as part of degradation mitigation efforts in the early design phases.

Under the prescribed driving conditions, the battery is not exerted much, and there is a net increase in SOC. The percent of the net energy that goes to charge the battery is about 1.6% of the total energy provided by the fuel cell. Thus, it is justified not to make any adjustment for changes in SOC when calculating hydrogen used for this preliminary analysis. If the parasitic power to operate ancillary devices in the fuel cell system and variations in utilization of hydrogen with power level are included, the increase in hydrogen consumption will be diminished as the upper-potential limit is lowered. This affirms that power management strategies and control strategies in the hybrid systems can be used to arrive at a trade-off between performance and degradation. Surrogate models are key enablers for this vision.

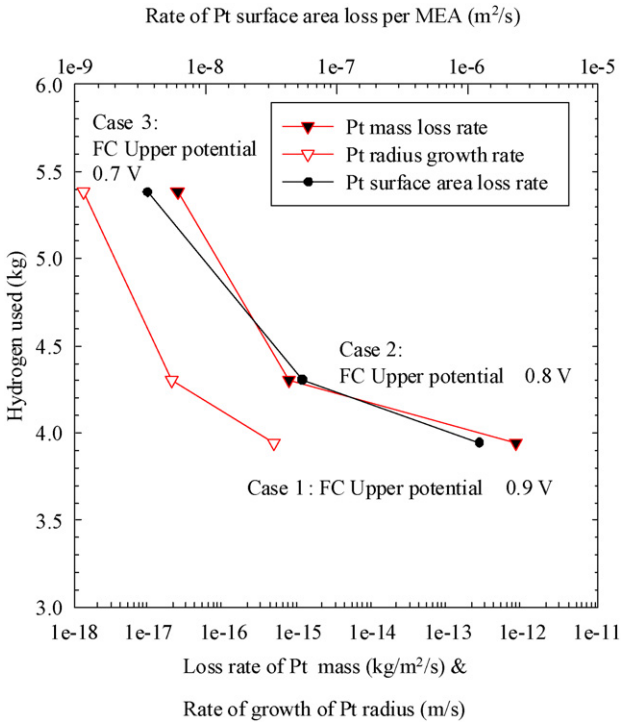

Fig. 3. Pt stability in PEMFC *vs.* hydrogen used (kg).

5. Response surface methodology (RSM) for surrogate life model of PEMFC

5.1. Need for RSM for fuel cell and battery life models

Present hybrid system models do not capture degradation phenomena associated with batteries and fuel cells. This is partly because a framework does not exist to make quantitative trades between life-time issues, performance, and cost in the conceptual and preliminary design phases. This can lead to designing the system principally focused on performance and capital cost. What is more, when efforts are made to incorporate life issues in system design at later stages, it actually becomes difficult to make large changes. Re-designing at this stage would require lots of effort in terms of time and cost. Neglect of life-time issues is also undesirable because of the costs associated with the loss of costly materials like Pt catalyst, Nafion® membrane in PEMFCs or those of lithium ion cell components. Moreover, system models without the incorporation of life models can lead to over prediction of performance in real time, which also creates safety concerns in case of an unexpected, early failure. Hence, it is paramount that life models are incorporated in hybrid system models. But detailed physics-based models are difficult to integrate with higher level system models, both in terms of different languages in which they are coded and also the variation in complexity levels. Another disadvantage is that complex physics-based life models require large computation time. Hence, simpler life models are desired that can be integrated in hybrid system model without losing much of the fidelity of the original physics-based models.

Surrogate models are a step in this direction. These models are important in the robust design strategy wherein the response of the system can be made less sensitive to noise factors. RSM is the tool used for this purpose. So far, surrogate models have been used for PEMFC performance [26] and compressor characteristics, [27] but not for degradation and durability phenomena in electrochemical energy storage and conversion devices. Moreover, the surrogate models developed by Tirnovan et al. are derived from experimental data and not from physics-based models. Though experimental data averts the need for the assumptions made with physics-based models, data derived from physics-based models are a necessity in situations where sufficient historical (or experimental) data are not available.

5.2. RSM—brief explanation of the methodology

RSM is a collection of statistical and mathematical techniques useful for developing, improving, and optimizing processes [28]. It provides a way to develop surrogate models for complex life models in a statistical framework. These surrogate models facilitate a robust design space solution. In robust parameter design methodology, product or process variations are reduced by choosing levels of controllable factors (or parameters) that make the system less sensitive (or robust) to changes in a set of uncontrollable factors. The simplest of response surface equations (RSEs) is a quadratic equation based on Taylor series approximation,

$$y = \beta_0 + \sum_{i=1}^{k} \beta_i x_i + \sum_{i=1}^{k} \beta_{ii} x_i^2 + \sum_{i=1}^{(k-1)} \sum_{j=i+1}^{k} \beta_{ij} x_i x_j + \varepsilon. \quad (2)$$

It is a multiple linear regression model with k—regressor variables. The Goodness of Fit procedures in statistics are used to test the surrogate model so obtained. Since these equations take much less computation time than the detailed physics-based model, probabilistic analyses of the system can be done relatively quickly.

5.3. Application of RSM to Pt catalyst dissolution

Among the degradation processes in PEMFCs, platinum catalyst dissolution and degradation is a major cause of loss of fuel-cell performance. Driving conditions such as idling (which results in the

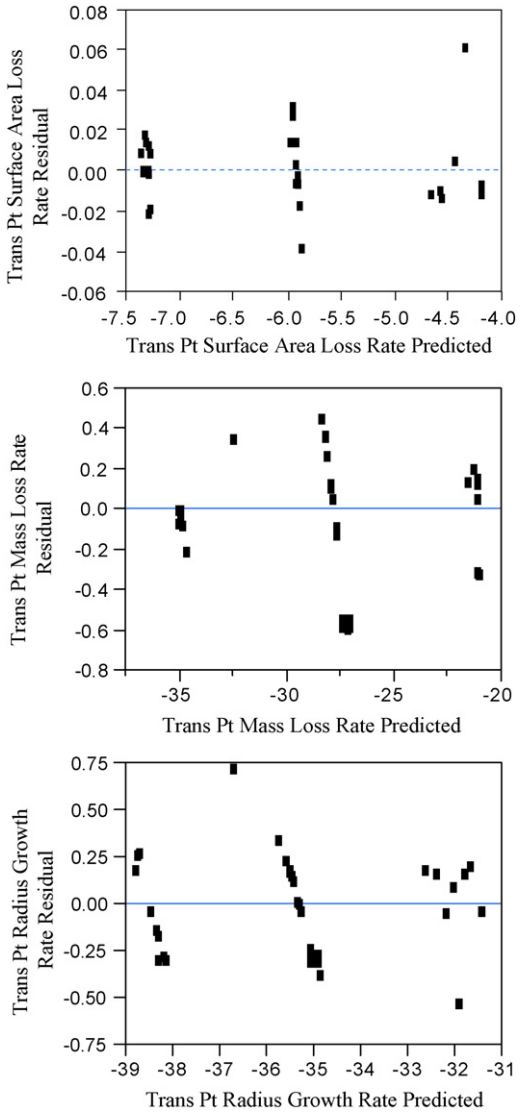

Fig. 4. Residual *vs.* predicted.

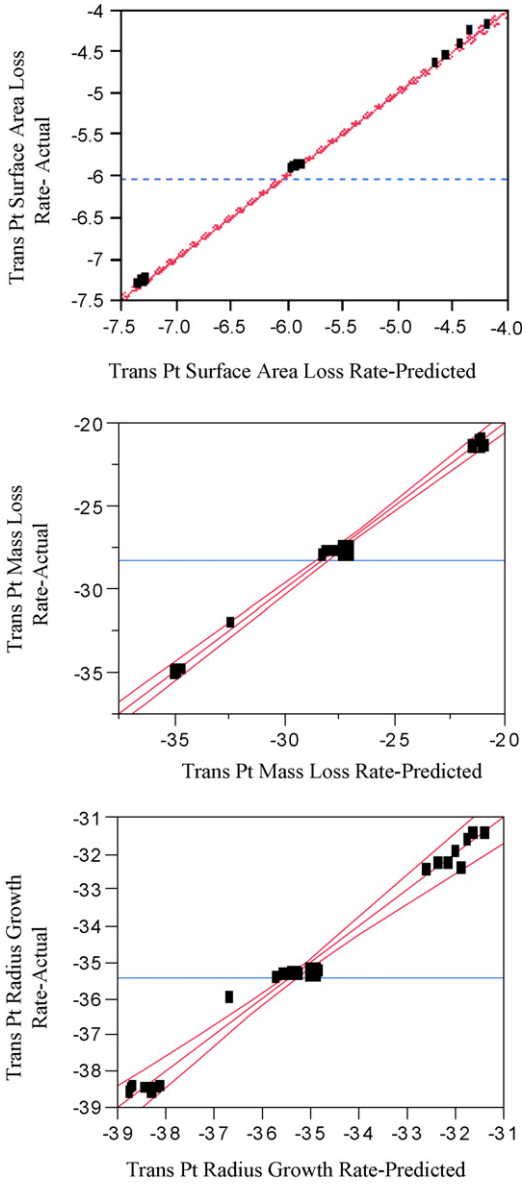

Fig. 5. Actual *vs.* predicted plot.

operation of PEMFCs at high potentials), city driving (which results in frequent potential cycles), or frequent starting and stopping of the fuel cell accelerate the Pt catalyst degradation processes. Hence, an effort is being made to develop surrogate model for Pt catalyst dissolution process.

Two variables that can be set in the control architecture are the upper and lower potential limits of the fuel cell. Other variables, such as the durations of the time step, and number of cycles (these variables define the driving schedule) are not known *a priori* and are in the hands of the driver. Additional variables, such as the particle size of the platinum catalyst, will have a distribution of values from the manufacturing processes. If the number of variables is large, a 2-level design of experiments is typically done to perform a screening analysis. The variables that have the most influence are then used to create RSEs.

In this initial study, just four variables are considered: upper and lower potential limits for the fuel cell, the number of cycles, and the time step. A square wave potential was used to generate the responses from the detailed physics-based model for platinum catalyst dissolution developed by Bi and Fuller [29]. Hence, the potential step in this case is simply the difference between the upper and lower fuel-cell potential. The responses from the model are the rates of platinum mass loss from the catalyst, reduction in electrochemical surface area, and growth in particle radii.

The upper and lower levels of each of the four variables were chosen as given in Table 3. Central Composite Design (CCD) of

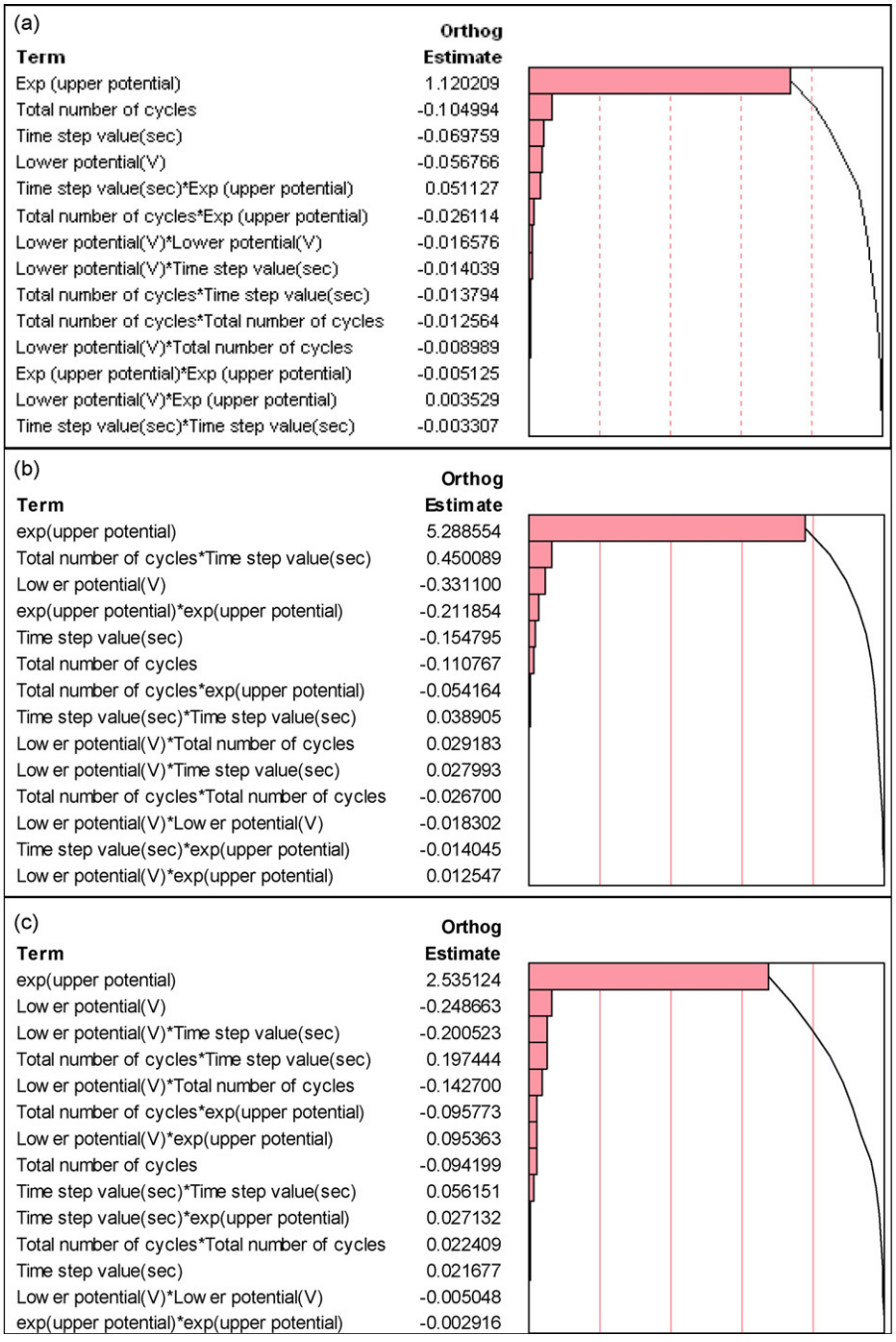

Fig. 6. Pareto plot for (a) Pt surface area loss, (b) Pt mass loss and (c) Pt particle radius growth rate (after transformation).

Table 3
Independent variables and the corresponding levels chosen for the surrogate model development

Variables	Upper level	Middle level	Lower level
Upper potential (V)	1	0.9	0.8
Lower potential (V)	0.7	0.6	0.5
Number of cycles	200	150	100
Time step (s)	60	35	10

Experiments was chosen to select the different cases to be run in the detailed model and obtain responses. Quadratic RSEs were created for each of the responses with the data obtained. A total of 32 "experiments" were run (27 cases were derived from Central Composite Design of Experiments and 5 extra cases were run using a time step of 25 s instead of the mid level of 35 s). The extra cases can not only help us increase the fidelity of the model but also lessen high correlation between independent variables when certain cases (outliers) have to be deleted. For the two cases with 200 cycles and 60 s time step, the physics-based model did not give any responses. The reason is that in the physics-based model with a bi-modal particle size distribution, as small particles dissolved their radii became vanishingly small. The associated shift in equilibrium potential with radius was so large that the particle surface completely oxidized before the completion of the simulation for these two cases [29]. It is acknowledged that the effect of creating the RSEs with less than two cases as required by CCD design will lead to some correlation between the independent variables. In this instance, we believe that the underlying physics-based model requires improvement, which is an on-going effort, and not a failing in the methodology proposed here.

5.4. Goodness of Fit tests

Since each response varied amongst different cases by orders of magnitudes, the responses were transformed from 'y' to 'exp (y)' before the RSEs were created. Moreover, the potential term in the Butler–Volmer equation highlights the exponential dependence of the Pt catalyst dissolution process in PEMFCs on cell potential. Hence, RSEs for the transformed metrics as a function of lower potential, number of cycles, time step and exponential of upper potential were obtained with $R^2 > 0.9$. The residual *vs.* predicted is shown in Fig. 4. The magnitude of the error is less than 2.5% of the predicted value for each of these responses, and the error distribution does not show any distinguishable pattern. However, the error distribution plot for the data points used for the development of RSEs, called the Model Fit Distribution (MFE), and the error distribution plot for the validation points (data points not used for surrogate model) showed high standard deviations and error ranges. Data points that cause a large variance, called outliers, were deleted. Ideally, no more than 7–8% outliers should be deleted to minimize correlation between the independent variables. In the present results, 10% of the outliers were deleted to reduce the error distribution. These indicate that the present surrogate model cannot fully replicate the dissolution process. Nonetheless, the framework is established for a PEMFC life surrogate model. One could observe data clumping in actual *vs.* predicted plot as seen in Fig. 5. Data clumping usually means that at the current settings, a single variable is driving the response.

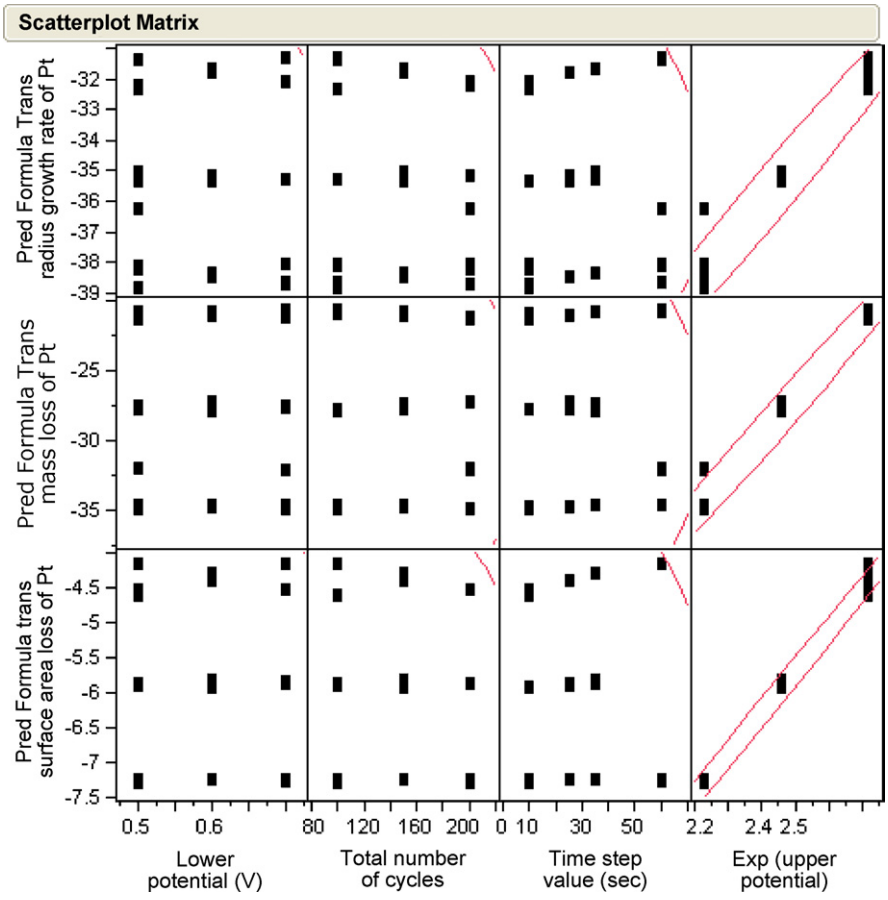

Fig. 7. Scatter plot matrix of the Pt catalyst dissolution metrics against the four independent variables.

5.5. Pareto plots and scatter plot matrix

To further analyze the sensitivity of the variability in response metrics to the independent factors, Pareto plots for all responses (Fig. 6) were created. The larger the value, the greater is the sensitivity of the results to that variable. These plots show that the "upper potential" contributes to more than 60% of the variability in the Pt catalyst dissolution responses in PEMFCs. Fig. 7 shows the scatter plot matrix between the independent variables and the metrics for the Pt catalyst dissolution process. The density ellipses for the metrics as a function of the upper potential, and also the random scatter of the data points for the metrics with respect to time step, number of cycles and lower potential also re-emphasize the dominant role of upper potential in the durability of PEMFC catalysts. These indicate that controlling the upper potential of the fuel cell in the hybrid system power management and control architecture is a positive direction towards addressing durability issues in PEMFC. The durability of the fuel-cell system may be improved by using fuel cell as a battery charger or range extender, and thus operating it only at relatively low potentials with a reduced number of starts and stops. Better RSEs will be developed in future to arrive at a robust design such that the degradation issues are made less sensitive to the uncertainties (not known *a priori*) associated with driving cycle such as time steps, number of cycles and potential steps and also to the variation in particle size distributions of the platinum catalyst particles. This work provided the framework for analysis, but other degradations mechanism for fuel cell durability, and cycle and calendar life of the battery pack will be included in future work.

6. Conclusions and future work

A framework for the surrogate model of Pt catalyst dissolution of PEMFC is developed. The effectiveness and importance of response surface methodology in electrochemistry degradation models is discussed. An indication about the relative importance of different variables that influence platinum catalyst dissolution is obtained and this knowledge could also be employed to design control architecture and power management strategies that help mitigate platinum catalyst degradation in hybrid systems and also to arrive at a trade-off between performance and degradation of the hybrid system. Better RSEs will be developed and integrated in the hybrid system model. A key enabler for developing more accurate RSEs will be a computationally efficient physics-based model for Pt degradation that takes into consideration different degradation mechanisms with minimal assumptions. The procedure and the methodology could also be extended to develop surrogate model for carbon corrosion in PEMFC from the electrochemistry models and also for the incorporation of battery degradation models in hybrid system framework. Ultimately, a robust design will evolve that makes the hybrid system less sensitive to uncertainties by controlling other independent variables and operating in a regime (through power management algorithms) that will be an optimized trade-off between different performance metrics and durability issues.

Acknowledgements

The authors extend their thanks to Dr. Dimitri Mavris and Dr. Tommer Ender from the ASDL at Georgia Tech for discussions regarding RSM. The authors would also like to acknowledge Dr. Gary Gray, Cheng Chen, Norimitsu Takeuchi and Tom Bradley for their comments on this work. Finally, the Georgia Tech Research Institute is gratefully acknowledged for financial support.

Appendix A

Vehicle design parameters:

Parameters	Value
Density of air, ρ_a (kg m^{-3})	1.2
Acceleration of gravity, g (m s^{-2})	9.81
Aerodynamic drag coefficient, C_d	0.26
Frontal area, F_{area} (m^2)	2.2
Coefficient of rolling resistance, C_{rr}	0.007

Vehicle model equations:

$$P_{d-total} = P_v + P_{rr} + P_{ad} + P_{acc}$$

$$P_v = m_v \times v \times a$$

$$F_{rr} = C_{rr} \times m_v \times g$$

$$P_{rr} = F_{rr} \times v$$

$$F_{ad} = \frac{1}{2} \times \rho_a \times v^2 \times C_d \times F_{area}$$

$$P_{ad} = F_{ad} \times v$$

$$P_{acc} = 1000\,\text{W}$$

$$m_{bv+pp} = 1450\,\text{kg}$$

$$m_v = m_{bv+pp} + m_b + m_{fc}$$

Maximum power demand = 110 kW

Symbol	Description
$P_{d\text{-}total}$	Total power demand of the vehicle (W)
P_v	Power demand of the vehicle due to vehicle velocity (W)
P_{rr}	Power to overcome rolling resistance (W)
P_{ad}	Power to overcome aerodynamic drag (W)
P_{acc}	Accessory power demand (W)
m_v	Net mass of the vehicle (kg)
v	Velocity of the vehicle (m/s)
a	Acceleration of the vehicle (m s^{-2})
F_{rr}	Force of rolling resistance (N)
F_{ad}	Force due to aerodynamic drag (N)
m_{bv+pp}	Base mass of vehicle +passenger payload (kg)
m_b	Mass of battery (kg)
m_{fc}	Net mass of fuel cell stack system (kg)

Appendix B

Fuel cell system design specifications

Compressed hydrogen tank pressure (MPa)	70
Weight of fuel cell stack/rated power (kg kW^{-1})	2.6
P_{fc_rated} (rated fuel cell power) (kW)	90
u_{H_2} (hydrogen utilization factor) (%)	90
A_{MEA} (area of 1 MEA of PEMFC) (cm^2)	200
m_{sub} (mass of FC subsystem) (kg)	150
Number of hydrogen tanks	4
Compressibility factor (Z)	1.57
Safety factor (to calculate hydrogen storage volume)	1.13
$m_{H_2\_tanks\_net}$ (net mass of all hydrogen tanks) (kg) (basis: http://www1.eere.energy.gov/hydrogenandfuelcells/pdfs/33098_sec3.pdf))	77.054
m_{H_2} (mass of hydrogen in tank at start of simulation) (kg)	5.4
MW_{H_2} (molecular weight of hydrogen) (kg mol^{-1})	0.002
F (Faraday's constant) (Coulombs mol^{-1})	96,485
n (for H_2)	2

N_{MEA} (number of PEMFC MEA needed) = 427

$$m_{fc} = 2.6 \times P_{fc\_rated} + m_{H_2\_tank} + m_{H_2} + m_{sub}$$

$$\text{Weight percent of hydrogen} = \frac{m_{H_2}}{m_{H_2} + m_{H_2\_tanks\_net}} = 6.54\%$$

$$\text{Hydrogen used} = \frac{1}{u_{H_2}} \int_0^t \frac{N_{MEA}\, i A_{MEA}}{n F\, MW_{H_2}}\, dt$$

Appendix C

Battery model equations:

$$OCP_{pos} = 4.19829 + 0.0565661 \tanh(-14.5546y + 8.60942) - 0.0275479 \left(\frac{1}{((.998432 - y)^{0.492465})} - 1.90111 \right) - 0.157123\, e^{(-0.04738y^8)} + 0.810239\, e^{(-40(y-0.133875))}$$

$0.4 < y < 0.9981$ [22]

$$OCP_{neg} = \frac{1.997 + 2.472 \times x}{1 + 31.823 \times x} \text{[23]}$$

$$OCP_{cell} = OCP_{pos} - OCP_{neg}$$

η_v = quadratic function of battery current density (assumed parameters)

$$V_{cell} = OCP_{cell} - \eta_v$$

Relation between state of charge of the battery and intercalation co-efficients of the individual electrodes:

During discharge process,

If anode is the limiting electrode,

$$SOC = \frac{x - x_{min}}{x_{max} - x_{min}}$$

and

$$y = (1 - SOC) \times (y_{max} - y_{min}) + y_{min}$$

If cathode is the limiting electrode,

$$SOC = \frac{y_{max} - y}{y_{max} - y_{min}}$$

Faraday's law used to update individual electrodes state of charge

$$m_b = w_{Li\text{-}cell} \times n_{Li}$$

$$\text{Energy of battery (J)} = \int_0^t V_{cell} \times n_{Li} \times I_{bat} \times dt$$

Variables	Description
y	Intercalation co-efficient of the positive electrode
x	Intercalation co-efficient of the negative electrode
OCP_{pos}	Open circuit potential of positive electrode (V)
OCP_{neg}	Open circuit potential of negative electrode (V)
OCP_{cell}	Open Circuit potential of individual cell (V)
η_v	Overpotential of individual lithium ion cell (V)
V_{cell}	Individual lithium ion cell voltage (V)
m_b	Net mass of the batteries in series (kg)

Battery design parameters:

Parameter	Value
Mass of one lithium ion cell ($w_{Li\text{-}cell}$) (kg)	0.908 (Yardney website)
Number of lithium ion cells (n_{Li})	53
y_{max}	0.9972
y_{min}	0.179
x_{max}	1
x_{min}	0.1
Initial state of charge	0.8 (variable input parameter)
Maximum Power from battery (P_{b_max}) (kW)	20
Capacity of individual lithium ion cell (Ah)	25

Appendix D

DC/DC converter model equation

$$y = 0.6077x^6 - 1.7325x^5 + 1.1629x^4 + 0.7525x^3 - 1.3222x^2 + 0.6276x + 0.8707$$

y : Fractional efficiency

x : Fraction of input power

Appendix E

Power sharing algorithm for the baseline model

If $P_{traction} >= 0$ & $P_{acc}>0$
  If $P_{traction} + P_{acc} > P_{FC\text{-}rated}$
    $P_{traction} + P_{acc} = P_{FC\text{-}rated} + P_{batt}$ (if battery has sufficient capacity)
  Else if $P_{FC\text{-}min} < P_{traction} + P_{acc} < P_{FC\text{-}rated}$
    If SOC >= 0.6
      $P_{traction} + P_{acc} = P_{FC}$
    Else if SOC <0.6
      $P_{traction} + P_{acc} + P_{batt\_charge} = P_{FC} = P_{FC\text{-}rated}$
    End
  Else if $P_{traction} + P_{acc} <= P_{FC\text{-}min}$
    If SOC <0.4
      $P_{traction} + P_{acc} + P_{batt\_charge} = P_{FC} = P_{FC\text{-}rated}$
    Else if 0.4<= SOC<0.45
      $P_{traction} + P_{acc} = P_{FC}$
    Else if 0.45<= SOC <1
      $P_{traction} + P_{acc} = P_{batt}$
    End
  End
Else if $P_{traction} < 0$ & $P_{acc}>0$
  If $P_{traction} + P_{acc} <0$
    If SOC <1
      $P_{batt\_charge} = P_{traction} + P_{acc}$
    End
  Else $P_{traction} + P_{acc} >0$
    If SOC >=0.7
      $P_{batt} = P_{traction} + P_{acc}$
    Else SOC <0.7
      $P_{FC} = P_{acc}$
      $P_{batt\_charge} = P_{traction}$
    End
  Else
    $P_{FC}=0$
    $P_{batt}=0$ (Battery discharge power for the accessories load and the battery charge power from regenerative braking are the same).
  End
End

Term	Explanation
$P_{traction}$	Traction power demand (W)
P_{acc}	Accessories power demand (W)
P_{FC_rated}	Rated fuel cell power (W)
P_{FC}	Fuel cell power (W)
P_{batt}	Battery discharge power (W)
P_{batt_charge}	Battery charge power (W)

References

[1] B. Johnston, M.C. Mayo, A. Khare, Hydrogen: the energy source for the 21st century, Technovation 25 (6) (2005) 569–585.
[2] K.T. Chau, Y.S. Wong, Hybridization of energy sources in electric vehicles, Energy Convers. Manage. 42 (9) (2001) 1059–1069.
[3] H.T. Yap, N. Schofield, C.M. Bingham, Hybrid energy/power sources for electric vehicle traction systems, IEEE Conference Publication 498(1) (2004), Power Electronics, Machines and Drives, 61–66.
[4] R. Kötz, M. Carlen, Principles and applications of electrochemical capacitors, Electrochim. Acta 45 (15/16) (2000) 2483–2498.
[5] P. Van den Bossche, F. Vergels, J. Van Mierlo, J. Matheys, W. Van Autenboer, SUBAT: an assessment of sustainable battery technology, J. Power Sources 162 (2) (2006) 913–919.
[6] W.G. Pell, B.E. Conway, Quantitative modeling of factors determining Ragone plots for batteries and electrochemical capacitors, J. Power Sources 63 (2) (1996) 255–266.
[7] T. Christen, M.W. Carlen, Theory of Ragone plots, J. Power Sources 91 (2) (2000) 210–216.
[8] G. Pede, A. Iacobazzi, S. Passerini, A. Bobbio, G. Botto, FC vehicle hybridisation: an affordable solution for an energy-efficient FC powered drive train, J. Power Sources 125 (2) (2004) 280–291.
[9] R.M. Darling, J.P. Meyers, Kinetic model of platinum dissolution in PEMFCs, J. Electrochem. Soc. 150 (11) (2003) A1523–A1527.
[10] J.P. Meyers, R.M. Darling, Model of carbon corrosion in PEM fuel cells, J. Electrochem. Soc. 153 (8) (2006) A1432–A1442.
[11] H.L. Tang, P.K. Shen, S.P. Jiang, F. Wang, M. Pan, A degradation study of Nafion proton exchange membrane of PEM fuel cells, J.Power Sources 170 (1) (2007) 85–92.
[12] C. Chen, G. Levitin, D.W. Hess, T.F. Fuller, XPS investigation of Nafion® membrane degradation, J. Power Sources 169 (2) (2007) 288–295.
[13] S.G. Chalk, Miller S J.F., Key challenges and recent progress in batteries, fuel cells, and hydrogen storage for clean energy systems, J. Power Sources 159 (1) (2006) 73–80.
[14] J. Vetter, P. Novák, M.R. Wagner, C. Veit, K.-C. Möller, J.O. Besenhard, M. Winter, M. Wohlfahrt-Mehrens, C. Vogler, A. Hammouche, Ageing mechanisms in lithium-ion batteries, J. Power Sources 147 (1/2) (2005) 269–281.
[15] P. Arora, R.E. White, M. Doyle, Capacity fade mechanisms and side reactions in lithium-ion batteries, J. Electrochem.Soc. 145 (10) (1998) 3647–3667.
[16] R. Spotnitz, Simulation of capacity fade in lithium-ion batteries, J. Power Sources 113 (1) (2003) 72–80.
[17] M.J. Kim, H. Peng, Power Management and design optimization of fuel cell/battery hybrid vehicles, J. Power Sources 165 (2) (2007) 819–832.
[18] W. Na, B. Gou, The efficient and economic design of pem fuel cell systems by multi-objective optimization, J. Power Sources 166 (2) (2007) 411–418.
[19] D.N. Mavris, D.A. DeLaurentis, O. Bandte, M.A. Hale, A Stochastic approach to multi-disciplinary aircraft analysis and design, AIAA98-0912, in: Presented at the 36th Aerospace Sciences Meeting and Exhibit, Reno, NV, January 12–15, 1998.
[20] J. Kim, S.-M. Lee, S. Srinivasan, C.E. Chamberlin, Modeling of proton exchange membrane fuel cell performance with an empirical equation, J. Electrochem. Soc. 142 (8) (1995) 2670–2674.
[21] C. Fellner, J. Newman, High-power batteries for use in hybrid vehicles, J. Power Sources 85 (2) (2000) 229–236.
[22] M. Doyle, J. Newman, A.S. Gozdz, Schmutz S C.N., J.-M. Tarascon, Comparison of modeling predictions with experimental data from plastic lithium ion cells, J. Electrochem. Soc. 143 (6) (1996) 1890–1903.

[23] G. Sikha, B.N. Popov, R.E. White, Effect of porosity on the capacity fade of a lithium-ion battery, J. Electrochem. Soc. 151 (7) (2004) A1104–A1114.
[24] P. Pei, M. Ouyang, Q. Lu, H. Huang, X. Li, Testing of an automotive fuel cell system, Int. J. Hydrogen Energy 29 (10) (2004) 1001–1007.
[25] http://www.epa.gov/otaq/sftp.htm.
[26] R. Tirnovan, S. Giurgea, A. Miraoui, M. Cirrincione, Surrogate model for proton exchange membrane fuel cell (PEMFC), J. Power Sources 175 (2) (2008) 773–778.
[27] R. Tirnovan, S. Giurgea, A. Miraoui, M. Cirrincione, Surrogate modeling of compressor characteristics for fuel-cell applications, Applied Energy 85 (5) (2008) 394–403.
[28] R.H. Myers, D.C. Montgomery, Response Surface Methodology, 2nd ed., Wiley, New York, 2002, pp. 1.
[29] W. Bi, T.F. Fuller, Modeling of PEM fuel cell Pt/C catalyst degradation, J. Power Sources 178 (2008) 188–196.